Structural investigation of bacteriorhodopsin and some of its photoproducts by polarized Fourier transform infrared spectroscopic methods-difference spectroscopy and photoselection

Karim Fahmy, Friedrich Siebert, and Paul Tavan*
Institut für Biophysik und Strahlenbiologie der Universität Freiburg, Albertstraße 23, D-7800 Freiburg i. Brsg.; and
*Physikdepartment T30, Technische Universität München, James-Franck-Strasse, D-8046 Garching, Germany

ABSTRACT The direction of selected IR-transition moments of the retinal chromophore of bacteriorhodopsin (BR) and functional active amino acid residues are determined for light- and dark-adapted BR and for the intermediates K and L of the photocycle. Torsions around single bonds of the chromophore are found to be present in all the investigated BR states. The number of twisted single bonds and the magnitude of these torsions decreases in the order K, L, light-adapted BR, dark-adapted BR. In the last, only the C_{14}—C_{15} single bond is twisted. The orientation of molecular planes and chemical bonds of such protein side chains, which are perturbed during the transition of light-adapted BR to the respective intermediates, are deduced and the results compared with the current three dimensional model of BR. Trp 86 and Trp 185 are found to form a rigid part of the protein, whereas Asp 96 and Asp 115 perform molecular rearrangements upon formation of the L-intermediate.

INTRODUCTION

The integral membrane chromoprotein bacteriorhodopsin (BR) of the plasma membrane of halobacteria halobium functions as a light-driven proton pump (for reviews see 1, 2). BR is organized as a hexagonal lattice in patches, which form the so-called purple membrane (PM). The retinal chromophore is covalently bound via a protonated Schiff base to lysine 216 of the 26-kD apoprotein. In its long-lived light-adapted state, absorption of a photon drives a photocycle which passes through the intermediates K (610 nm), L (550 nm), M (410 nm), N (550 nm), and O (640 nm), distinguishable by their visible absorption (3). The photocycle, coupled to the proton motive steps, is completed within ~30 ms at room temperature. The comparison of the vibrational spectra of retinal in BR and its intermediates with spectra of known isomers of retinal and its Schiff bases has been used to determine the protonation and isomeric states of the chromophore (4–6). From the vibrational analysis, it is known that the chromophore is all-*trans* in light-adapted BR (BR_{568}), 13-*cis*,15-syn in BR_{548} (~40% of dark-adapted PM), 13-*cis*,15-anti in K, L, M and N. Only in M, the Schiff base is deprotonated.

In a recent study, we applied polarized FTIR-difference spectroscopy to light-adapted BR and to its photoproducts K and L (7). A formalism has been developed to obtain the angle Φ between the IR-transition moment (M_{ir}) of an absorption band and the electronic transition moment of the retinal chromophore, using difference spectra that were induced by polarized actinic light. From those data, combined with quantumchemical calculations, the plane of the retinal chromophore was found to be perpendicular to the plane of the PM. In addition, our results showed that the orientations of IR-transition moments of hydrogen-out-of-plane (HOOP) vibrations of the chromophore depend sensitively on single bond twists in the polyene moiety. Our model calculations have demonstrated that such twists induce a vibrational coupling of HOOP modes with deformation modes of the carbon skeleton. Thus, if single bonds adjacent to a certain ethylenic unit of the polyene chain are twisted, dipoles of HOOPs localized at that unit become bent towards the ethylenic plane, i.e., they loose their out-of-plane orientation. Because for protonated retinal Schiff bases vibrational dipoles of deformation modes generally are much larger than those of HOOPs, small coupling induced by twists as small as 15°–30° suffice to produce seizable effects. According to the calculations larger twists can lead to complete loss of out-of-plane character for HOOP vibrational dipoles (for a discussion of computational methods, reliability of results et cetera, see 8). Therefore, geometrical implications derived from HOOP modes are valid only if photoselection data actually prove the out-of-plane character of their IR transition moments. Our data have shown that in many cases the vector of a HOOP transition exhibits a considerable component along the electronic transition moment, i.e., along the long axis of retinal. Even complete alignment of HOOP transition moments with the retinal axis was observed.

According to these results, a "rule of thumb" may be formulated for the interpretation of polarized FTIR

Address correspondence to Dr. F. Siebert.

0006-3495/91/11/989/13 $2.00

data of HOOP modes as follows: "if photoselection data prove that a transition moment of a localized HOOP mode is actually perpendicular to the retinal axis then the orientation of the corresponding ethylenic unit can be determined; in contrast, localized HOOP modes, which exhibit components along the electronic transition moment are indicative for torsions around single bonds neighboring the units." In BR such twists can be enforced by the protein environment and have been considered crucial for alterations in the Schiff base pK (9).

In this study, mainly the spectral range between 720–1,020 cm^{-1} (typical of HOOP vibrations of polyenes) has been investigated by polarized room and low temperature FTIR-difference spectroscopy combined with polarized excitation (photoselection) of the PM to the respective intermediate. Our interest has been to demonstrate the validity of dichroic studies of retinal HOOP vibrations to localize single bond torsions, to support HOOP assignments deduced from isotopically labeled compounds and to monitor part of the chromophore's relaxation after the primary photoisomerization. In addition, we have drawn structural conclusions from the polarized data of vibrational modes that have been assigned to amino acid residues.

Photoselection experiments in context with polarized FTIR difference spectroscopy have already been carried out on the BR-M transition (10) so that we have focussed on the K, L and dark-adapted state of BR, as N and O are difficult to gain access to by our methods at present. IR-dichroic data of the BR-K, BR-L and BR-M transition (after unpolarized excitation), which allow the evaluation of the angle θ between M_{ir} and the PM-normal, have been reported (7, 11, 12). Such measurements have been repeated in this study. Thereby, both Φ and θ values could be given for all the IR-transition moments investigated.

MATERIALS AND METHODS

Purple membranes from *Halobacterium halobium* were isolated, bleached and regenerated with labeled retinals as described (13, 14). The isotopically labeled retinals were synthesized as described (15, 16). 200 μg PM were dried from a suspension onto an AgCl window to form a hydrated BR-film. The way to obtain anisotropic photoconversion of the BR-film to the K and L state by use of polarized actinic light (i.e., photoselection) has been described (7). Light–dark-adaptation difference spectra were recorded at 280 K. A previously dark-adapted sample (kept in the dark for at least 18 h) was illuminated within the FTIR-spectrophotometer by polarized light with wavelengths >500 nm. In all experiments an IR-polarizer was mounted in front of the sample chamber but could be removed to allow for illumination of the sample. The polarizer was switched by a step motor to select IR-light which was polarized parallel or perpendicular to the polarization of the actinic light. For both polarizations, groups of 400 scans were accumulated alternately before and after the polarized illumination, respectively. Scans that belonged to the same IR-polarization after the illumination were ratioed against those before it to obtain the polarized IR-difference spectra A_h^p and A_v^p in which the measuring IR-beam was polarized parallel and perpendicular to the polarization of the actinic light. Stability of the spectrophotometer usually allows to sum up four groups of scans so that a polarized spectrum derives from 1,600 scans. At least four spectra of this type were added to obtain an acceptable signal to noise ratio in the dichroic difference spectrum which is defined as $A_h^p - A_v^p$.

Quantitative evaluation of directions of IR-transition moments

The methods of quantitative evaluation of the measured IR dichroism in photoselection experiments have been reported in detail (7). Due to the experimental setup (direction of polarized actinic light and polarized IR-light are perpendicular to the sample), only those components of the electronic and the IR-transition moments contribute to absorption that lie in the plane of the sample. Therefore, the abbreviations m_{ir} and m_{el} denote the in plane components of the IR- and the electronic transition moment, respectively. Consequently, Φ lies in the plane of the sample, i.e., in the plane of the PM. The angle Φ can be derived from the dichroic difference by the relation

$$\tan^2\Phi = \frac{m_{yo}^2}{m_{xo}^2} = \frac{m_{ir}^2 - (m_{xo}^2 - m_{yo}^2)}{m_{ir}^2 + (m_{xo}^2 - m_{yo}^2)} = \frac{A - c(A_h^p - A_v^p)}{A + c(A_h^p - A_v^p)}, \qquad (1)$$

m_{xo} and m_{yo} are the components of m_{ir} in the plane of the sample for a molecule with the in plane component of its electronic transition moment parallel to the polarization of the actinic light. The absorption A is the sum of A_h^p and A_v^p which coincides with an unpolarized measurement of the absorbance changes. The constant c is a factor which enlarges the measured dichroic difference so that it corresponds to an idealized photoselection experiment. This correction is necessary for several reasons: (*a*) the best anisotropy which can be achieved by polarized illumination is described by a $\cos^2\delta$ distribution function where δ denotes the angle between m_{el} and the vector of the electric field of the actinic light. Therefore, the photoselection is not ideal in the sense that also such molecules will be photoconverted for which δ is different from zero. (*b*) Because the photoconversion is evoked at low temperature, the photoproduct accumulates as a function of illumination time. This causes a reduction of the induced anisotropy because of the increasing number of photoreacted molecules with $\delta > 0$. (*c*) Loss of polarization of the actinic light due to scattering in the sample further reduces the induced anisotropy. The factor c is independent of the wavenumber but differs for each experiment, because it is a function of the amount of photoconversion.

There are two ways to relate the measured dichroic differences to the hypothetical result which would be obtained if 100% of the sample was photoconverted with m_{el} of each molecule being oriented parallel to the electric field vector of the polarized actinic light. The first method relies on a "standard IR-vibration" (with absorbance AS) for which m_{ir} is known to be parallel to m_{el} of the retinal chromophore. For this mode $\tan^2\Phi$ equals zero. Therefore, $c = AS/(AS_h^p - AS_v^p)$. As c is independent of the wavenumber, the obtained value serves to produce the ideal result for all absorption bands just by multiplying the measured dichroic difference spectrum by this factor. However, if nothing is known about the orientation of any m_{ir}, c can be evaluated by measuring the dichroic difference of an arbitrarily chosen absorption band as a function of the amount of photoconversion (7). By this procedure we have shown that Φ of the C=C stretching vibration of BR at 1,527 cm^{-1} is zero. Therefore, we use the C=C stretching mode as "standard IR-vibration" in the present paper. Consequently, all the processes which render the photoselection less than ideal are corrected for. (Polarization losses of the measuring IR-beam can be neglected. This is because no intensity was measured when an analyzer was mounted behind the sample in crossed orientation to the polarizer.)

The constant c has been incorporated into the figures as a scaling factor which renders the absorption band of the C=C stretching mode of BR at 1,527 cm^{-1} in the dichroic difference spectra as large as in the corresponding unpolarized measurement. After this scaling, which is ~7–10 depending on the achieved photoselection, only the spectral noise contributes to the uncertainty in the presented Φ-values in Table I. However, for a given signal to noise ratio, the error is larger if Φ is close to 0° or 90° as compared to angles near 45°. This is due to the trigonometric function in Eq. 1. The errors indicated in Table I were obtained in the following way. The amount of noise in the difference bands was estimated and the influence on the solution of Eq. 1 evaluated. For the dichroic difference bands below 900 cm^{-1}, which are as small as 0.0001 absorbance units, up to 30% is noise. This produces an error of ±8° for a mode with a true value $\Phi = 45°$. This error range is indicated by " ~ ." However, a gain of accuracy due to larger signals as is the case above 900 cm^{-1} is often counterbalanced by the behaviour of the trigonometric function in Eq. 1 for Φ-values > 80° and < 10°. In this range, Φ is a steep function of the dichroic difference. Only for seven of 22 evaluations of absorption bands the signal was large enough and Φ outside the critical range to allow more certainty. In these cases, variation of the dichroic difference by the estimated amount of noise yields errors within ±4°.

Because the orientation of M_{ir} is only partially described by the angle Φ, a second set of measurements of the IR-dichroism was carried out in which the plane of the sample was tilted so that the normal of the PM forms an angle $\alpha > 0°$ with respect to the incident IR-beam. This allows the determination of the angle θ between M_{ir} and the normal of the PM (7, 11, 17). The evaluation is based on the dichroic ratio (i.e., the absorbance ratio) of the corresponding band observed with IR-polarization in the plane of incidence and perpendicular to it, respectively. The nomenclature is A_h for the difference spectrum recorded with IR-polarization in the plane of PM and A_v with the IR-polarization tilted with respect to the normal of PM. The angle θ is derived from the dichroic ratio R by the relation

$$R = \frac{A_v}{A_h} = 1 - \frac{3\langle p_2\rangle \sin^2\alpha}{n^2(1 - \langle p_2\rangle)} \quad \text{and}$$
$$p_2 = \frac{3\cos^2\theta - 1}{2}, \qquad (2)$$

where $\langle p_2\rangle$ denotes the integration over θ from 0 to π of the unknown orientational distribution function $f(\theta)$ multiplied by p_2. Therefore, $\langle p_2\rangle$ is the weight of the second Legendre polynomial in the representation of $f(\theta)$ by a sum of even Legendre polynomials (11). From this term, θ is obtained. Contributions of the orientational disorder of PM patches to $f(\theta)$ are not accounted for because they influence the resulting values of θ less than the uncertainty which is caused by the spectral noise. A refractive index $n = 1.7$ is assumed (18). Based on Eq. 2, the discrimination of θ-values between 80° and 90° by the corresponding dichroic ratios is difficult. Therefore, the lower limit of 80° is given for modes which are mainly polarized in the plane of the PM. The accuracy of θ-values below 80° is mainly determined by the signal to noise ratio. The direct division of peak intensities in order to determine R produces large errors, due to the uncertainty of the base line position in the difference spectra. Therefore, R was determined as the slope of a linear regression of the absorption band in A_v versus A_h which is independent of any different offsets in the spectra. The remaining error limits were estimated as in the case of photoselection measurements. The determination of the tilt angle α was done by adjusting it to some positive value, measuring the corresponding dichroism of the amide I and amide II absorption bands and then looking for a negative value of α, which causes the same dichroic ratios in both bands as is the case for the positive one. The so defined pair of α-values is symmetric with respect to the zero point of the scale of tilt angles. This calibration is based on the true optical axis of the spectrophotometer, thereby independent of any mechanical prealignment of moveable parts of the sample holder. In addition, the signal to noise ratio of the involved absolute absorption bands of the amide I and II modes is ~30-fold larger than that of the evaluated difference bands. Therefore, any remaining uncertainty in the determination of α can be neglected as compared with the described errors in the evaluation of the difference spectra.

RESULTS

Evaluation of Φ-values in the spectral range of HOOP vibrations

The most intense HOOP vibrations are found in the photoproduct K of the BR-photocycle. The corresponding BR-K difference spectrum recorded with unpolarized IR beam is dominated by positive bands at 974, 956,

TABLE I Frequencies (in cm^{-1}) of the evaluated vibrations and orientation of the corresponding IR-transition moments

BR_{570}	Φ; θ	BR_{548}	Φ; θ	K	Φ; θ	L	Φ; θ	Assignment
971*	~85°; >80°	968*	~85°; >80°	974	<12°; >80°	968	~85°; >80°	C_7=C_8 HOOP‡
959*	45°; >80°	956*	>70°; >80°	956	<12°; >80°	951	45°; >80°	C_{11}=C_{12} HOOP§
/		800*	17°; >80°	/		/		C_{14} HOOP§
1,740	70°; 41°	/		/		1748	~45°; 37°	Asp 96[a]
1,733	68°; 55°	/		/		1727	~45°; 44°	Asp 115[a]
833	~80°; >80°	/		829	~80°; >80°	/		Tyr 185[b]
757	~45°; 36°	/		/		751	~45°; 43°	Trp[c]
742*	62°; 46°	746*	62°; 46°	746	~90°; 49°	746	~45°; 37°	Trp 86[d]
742‖	~45°; 33°							

Φ: angle between m_{ir} and m_{el}; θ: angle between M_{ir} and normal PM (for definitions see materials and methods). The assignments of the C_{11}=C_{12} and C_{14} HOOP vibrations in light and dark-adapted BR are taken from (20, 21). Only the predominant mode character is represented. The assignments of protein modes are those of (*a*) 36, (*b*) 25, (*c*) 24, and (*d*) 23. *measurement at 280 K, all other data from measurements at 170 K and below. ‡assignment taken from (37). §mode character confirmed by FTIR-difference spectra using PM regenerated with labeled retinals; ‖measurement at 80 K; ~ uncertainty ± 8°; in all other cases ± 4° (see materials and methods).

and 942 cm^{-1} (Fig. 1 *a*). Less intense but distinct peaks are observed at 811 and 804 cm^{-1}. These bands reflect an increase in IR-absorption. The corresponding decrease which belongs to the depletion of light-adapted BR upon K-formation is not seen, due to the large positive absorption. The described absorption bands are also seen in resonance Raman spectra of the K-intermediate (19). Therefore, they are caused by chromophore vibrations. From the weaker difference bands only the absorptions at 742/746 cm^{-1} and 833/827 cm^{-1} are evaluated. They are caused by amino acid residues. A more detailed discussion and references of band assignments are given below (for an survey see Table I).

We now consider the orientation of the IR-transition moments of selected vibrations with respect to the polarization of the actinic light. The orientation is given as the angle Φ between the projections of the IR-transition moment M_{ir} and the optical transition moment M_{el} of the chromophore (in light-adapted BR) onto the plane of the sample, i.e., the plane of PM. The so defined vector components are denoted as m_{ir} and m_{el}, respectively. The evaluation of Φ is based on the dichroic difference $A^{p}_{h} - A^{p}_{v}$. An absorption band with $\Phi < 45°$ keeps its sign as compared to an unpolarized measurement (i.e.,$A^{p}_{h} + A^{p}_{v}$). If $\Phi = 45°$ the corresponding band does not show up in the dichroic difference, because $A^{p}_{h} = A^{p}_{v}$. In the case of $\Phi > 45°$, the band changes its sign in the dichroic difference as compared to the unpolarized spectrum. The dichroic differences are normalized with respect to the C=C stretch mode of light-adapted BR at 1,527 cm^{-1} to relate band intensities to those of the unpolarized experiment. This normalization accounts for the complete polarization of m_{ir}(C=C stretch) along m_{el} (7) (see also materials and methods). The CH_3-rocking mode at 1,009 cm^{-1} can serve as an internal standard to compare intensities in the FTIR-difference spectra of different intermediates, because m_{ir}(CH_3-rock) is equally well polarized along m_{el}.

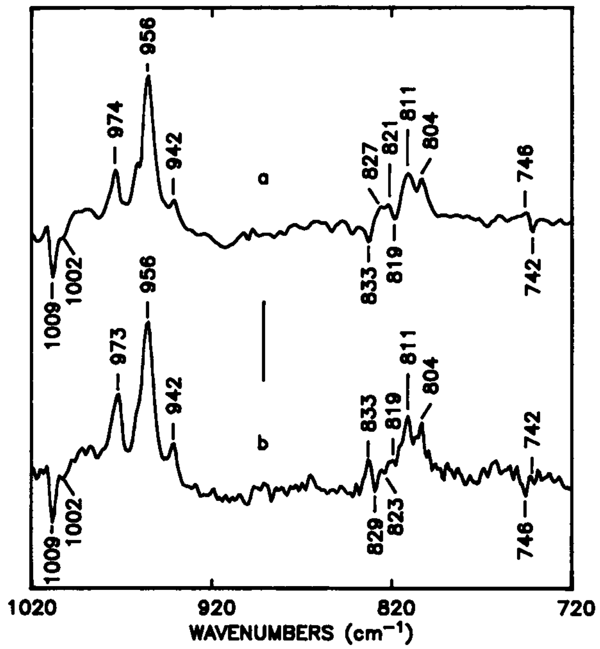

FIGURE 1 BR-K difference spectra at 80 K in H_2O, induced by light with wavelengths between 495 and 550 nm. (*a*) Unpolarized measurement. Bands of the K-intermediate show upwards, those of unphotolyzed BR_{528} downwards. (*b*) Dichroic difference spectrum (see Materials and Methods) normalized to the spectrum in (*a*) with respect to the ethylene absorption of BR_{568} at 1,527 cm^{-1} (not shown). Bands with their IR-transition moments polarized parallel to the electronic transition moment have the same size and intensity as in (*a*). Bands with their transition moments polarized perpendicular to the electronic transition moments change their sign as compared to (*a*). The bar indicates an absorption change of 3* 10^{-3} and 3.7* 10^{-4} absorbance units in *a* and *b*, respectively.

Fig. 1 shows the dichroic difference (*b*) of the BR-K spectrum in comparisons with the unpolarized measurement (*a*). All the above mentioned chromophore bands are visible in Fig. 1 *b* with almost the same intensity as in Fig. 1 *a*, arguing for a small angle Φ. From the quantitative evaluation of the bands $\Phi < 12°$ is obtained. Due to overlap with the BR-absorption (underlying negative bands), we can only give this upper limit for Φ. The absorption bands of the protein exhibit clearly different polarizations as compared to those of the chromophore. The difference band at 833/829 cm^{-1} in Fig. 1 *a* completely changes its sign in Fig. 1 *b*. Therefore, m_{ir} of both the BR (833 cm^{-1}) and the K-vibration (829 cm^{-1}) exhibit large components perpendicular to m_{el} ($\Phi = 80°$). The same holds for the small neighboring difference band at 819/821 cm^{-1}, the assignment of which is not clear as yet. For the BR absorption at 742 cm^{-1} we obtain $\Phi = 45°$ because the band has disappeared in Fig. 1 *b*. However, the corresponding m_{ir} in K which causes the absorption at 746 cm^{-1} (Fig. 1 *a*) is polarized perpendicular to m_{el} as evidenced by its inversion in Fig. 1 *b*.

During the BR-L transition the spectral changes in the range between 720 and 1,020 cm^{-1} (Fig. 2 *a*) are less pronounced than in the BR-K difference spectrum and, therefore, a lower signal to noise ratio results. In particular, the difference bands are due to frequency shifts rather than to increased absorption intensities as is mainly the case for the BR-K transition. The strongest difference band is the chromophore absorption change from 959 cm^{-1} in light-adapted BR to 951 cm^{-1} in L. This band cancels in the subtraction of both spectra and is not seen in Fig. 2 *b*. This indicates $\Phi = 45°$. According to the arguments presented above, the chromophore vibration that causes the 971/968 cm^{-1} difference band corresponds to $\Phi = 85°$ in both BR_{568} and L-intermediate.

The 742/746 cm^{-1} band of the protein loses nearly all

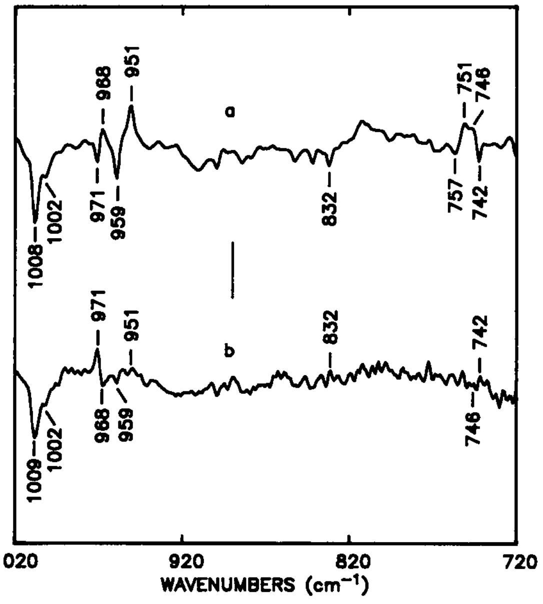

FIGURE 2 BR-L difference spectrum at 170 K in H_2O, induced by light with wavelengths above 610 nm. (*a*) Unpolarized measurement. Bands of the L-intermediate show upwards (conventions as in Fig. 1). (*b*) Dichroic difference spectrum. The bar indicates an absorption change of 2* 10^{-3} and 2.2* 10^{-4} absorbance units in *a* and *b*, respectively.

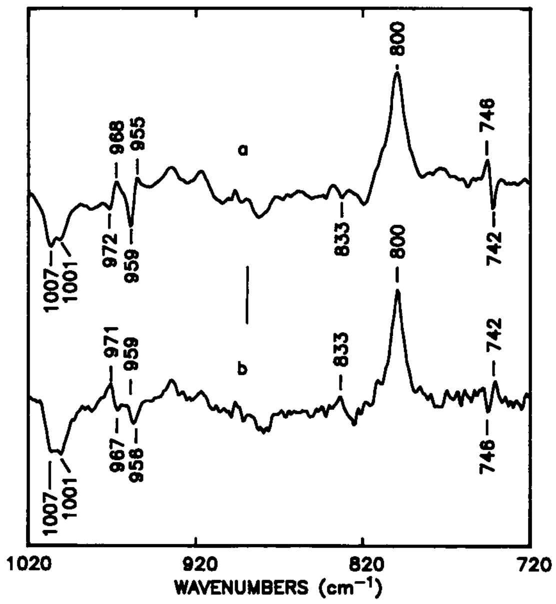

FIGURE 3 Light/dark-adaptation difference spectrum of BR at 280 K in H_2O, induced by polarized light with wavelengths above 495 nm. (*a*) Unpolarized measurement. Bands of the dark-adapted state show upwards (conventions as in Fig. 1). (*b*) Dichroic difference spectrum. The bar indicates an absorption change of 2* 10^{-3} and 3.3* 10^{-4} absorbance units in *a* and *b*, respectively.

its relative intensity in Fig. 2 *b* as compared to Fig. 2 *a*. Therefore, m_{ir} of this mode in BR as in L forms an angle Φ of about 45° with m_{el}. The neighboring protein difference band at 757/751 cm^{-1} is characteristic for the BR-L transition. It seems to cancel in the dichroic difference at least to the noise level and we estimate Φ of this mode remains at about 45° during the BR-L transition. The protein absorption of light-adapted BR at 833 cm^{-1} is hardly resolved in the BR-L measurement. Therefore, the corresponding Φ values were not evaluated.

In the difference spectrum of light–dark-adaptation in Fig. 3 *a*, the predominant peak is found at 800 cm^{-1} and reflects a large absorption increase of a chromophore vibration in the 13-*cis*,15-syn isomer of retinal in dark-adapted BR (BR_{548}). The band has the same sign in the dichroic difference in Fig. 3 *b*. This shows that m_{ir} of this mode is almost parallel to m_{el} ($\Phi = 17°$). In contrast, the less intense absorption bands at higher frequencies are again typical difference bands. In agreement with the BR-L data, the 972/968 cm^{-1} absorption difference is caused by a mode with m_{ir} perpendicular to m_{el}. Also, m_{ir} of the BR-absorption at 959 cm^{-1} is again found to deviate by 45° from m_{el}. However, m_{ir} of the corresponding HOOP mode in the 13-*cis*,15-syn chromophore of BR_{548} is polarized nearly perpendicular to m_{el}, because a negative band at 956 cm^{-1} is present in the dichroic difference in Fig. 3 *b*. Due to the overlap with the BR-absorption at 959 cm^{-1} in the unpolarized measurement, Φ can only be estimated to be $> 70°$.

Both the protein modes of light-adapted BR at 833 and 742 cm^{-1} possess large angles Φ ($\sim 80°$ and 62°, respectively) as evidenced from the inversion of the bands in Fig. 3 *b* as compared to Fig. 3 *a*. This result differs from the orientation of m_{ir} of the 742 cm^{-1} vibration when measured at low temperatures. At 280 K, Φ is $\sim 20°$ larger than at 170 K (BR-L transition) and 80 K (BR-K transition). Upon dark-adaptation, this polarization is conserved for the 746 cm^{-1} vibration in BR_{548}. For the vibration of BR_{568} at 833 cm^{-1}, the corresponding position in the 13-*cis*,15-syn chromophore cannot be denoted unambiguously. Therefore, no value for Φ can be given.

Evaluation of θ-values in the spectral range of HOOP vibrations

The difference spectra shown in the following section were induced by unpolarized actinic light and measured with polarized IR-radiation. The plane of the sample was tilted with respect to the incident IR-beam. This allows the mean angle θ between M_{ir} and the sample normal to be obtained (see materials and methods). The latter is also denoted as z-axis. We focussed on the BR-L transition and the light–dark-adaptation. Our results on the linear dichroism of the BR-K difference spectra (data not shown) agree with those reported by (11).

Fig. 4 shows A_h and A_v of the BR-L transition in the upper and lower trace, respectively. For the bands above 900 cm^{-1}, M_{ir} is oriented in the plane of the PM ($\theta > 80°$) which is visualized by the decrease of their intensity of A_v. The changes in the intensities near 750 cm^{-1} are more complicated. The dichroic ratio is best determined from difference spectra as the slope of a linear regression line of both spectra in the frequency range of interest. This is shown in Fig. 5. The slope of the line obtained from the band at 742 cm^{-1} is considerably smaller than that corresponding to the absorption of the photoproduct at 746 cm^{-1}. One might suspect a reorientation of M_{ir} of this mode, changing from an orientation parallel to the plane of the PM in BR_{568} (causing the smaller slope which suggests $\theta = 90°$) to an orientation with a considerable z-component in L-intermediate ($\theta = 38°$). Contrarily, the 757/751 cm^{-1} vibration is a mode with a large z-component ($\theta \sim 40°$) in both BR_{568} and L. For the absorption at 832 cm^{-1}, no straight regression line was obtained, and therefore no angle θ has been evaluated.

The difference spectra of light–dark-adaptation are shown in Fig. 6. With one exception, all bands are larger when observed with IR-polarization perpendicular to the plane of incidence, i.e., in the plane of the PM (Fig. 6 *a*). This indicates small components of the corresponding IR-transition moments along the z-axis. Only the 742/746 cm^{-1} difference band is slightly larger in Fig. 6 *b* as compared to Fig. 6 *a* and, therefore, M_{ir} of this mode has a considerable z-component. The corresponding linear regression is shown in Fig. 7. An angle $\theta = 46°$ between M_{ir} and the z-axis is obtained for both the BR_{568} and BR_{548} vibration. In contrast, the HOOP-vibrations of the chromophores are again polarized in the plane of the PM ($\theta > 80°$). Table I summarizes the θ values of the difference bands in the K and L-intermediates.

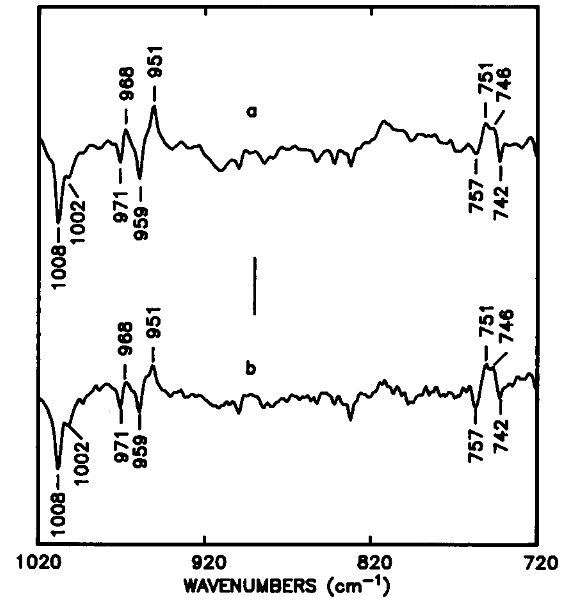

FIGURE 4 BR-L difference spectrum at 170 K in H_2O induced by unpolarized light with wavelengths above 610 nm and recorded with polarized IR-beam. Spectral range of HOOP vibrations. The plane of the sample was tilted 50° with respect to the incident IR-beam. (*a*) A_h-spectrum; (*b*) A_v-spectrum. The bar indicates an absorption change of 2* 10^{-3} absorbance units.

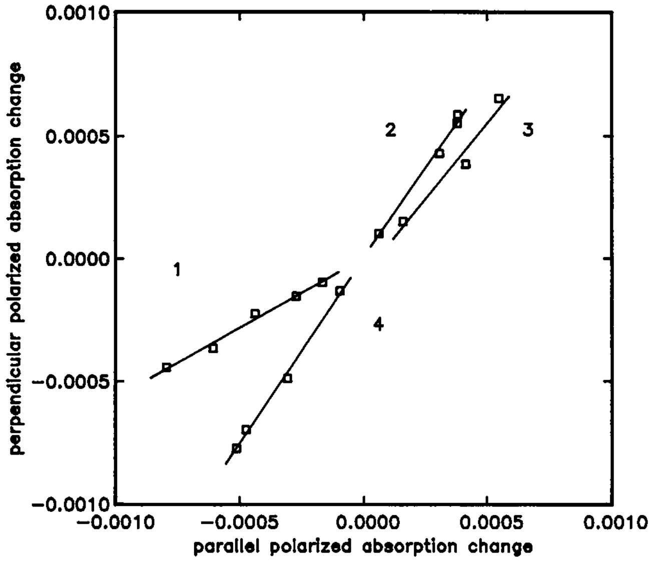

FIGURE 5 Linear regressions of the absorption intensities of the Trp 86 difference band at 742/746 cm^{-1} and the second Trp difference band at 757/751 cm^{-1} in the BR-L difference spectra shown in Fig. 4. x-axis: intensities taken from the spectrum with IR-polarization perpendicular to the plane of incidence (A_h-spectrum). y-axis: intensities taken from the spectrum with IR-polarization in the plane of incidence (A_v-spectrum). The slopes in the indicated spectral ranges define the following dichroic ratios R: 1: $R = 0.60$ (739–742 cm^{-1}); 2: $R = 1.52$ (744–747 cm^{-1}); 3: $R = 1.27$ (751–753 cm^{-1}); 4: $R = 1.56$ (754–757 cm^{-1}).

Orientation of IR-transition moments in the spectral range of carbonyl stretching frequencies

In addition to the low frequency range of the spectra, we have investigated the 1,800–1,660 cm^{-1} region in the BR-L transition (Fig. 8) to evaluate vibrations which are caused by the protein. Two C═O stretching vibrations of protonated carboxylgroups contribute to the spec-

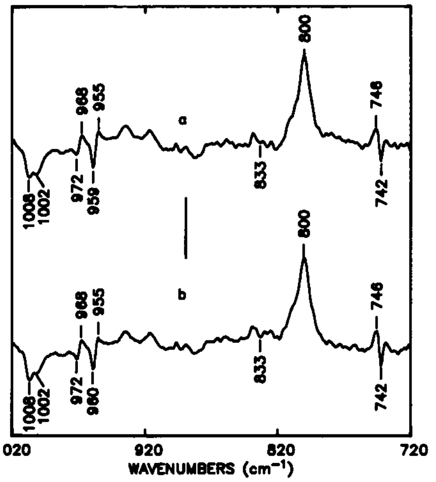

FIGURE 6 Light/dark-adaptation difference spectrum of BR at 280 K in H_2O, induced by unpolarized light with wavelengths above 495 nm and recorded with polarized IR-beam. Bands of the 13-*cis*,15-syn state show upwards, those of light-adapted BR downwards. The plane of the sample was tilted by 30° with respect to the incident IR-beam. (*a*) A_h-spectrum; (*b*) A_v-spectrum. The bar indicates an absorption change of $3*10^{-3}$ absorbance units.

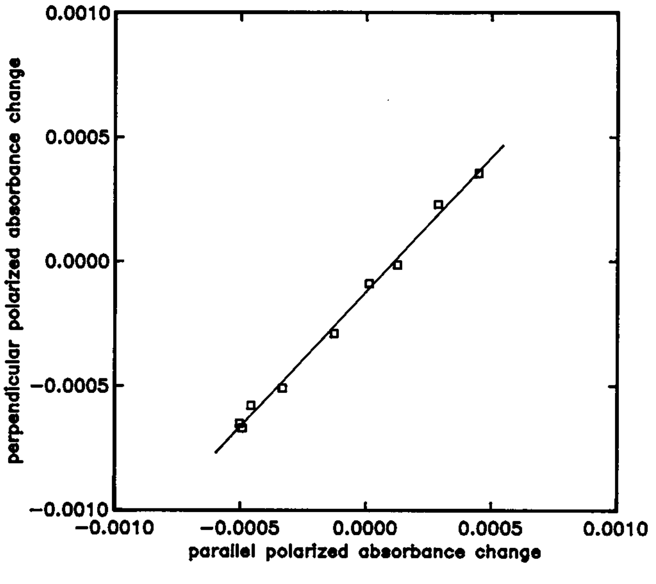

FIGURE 7 Linear regression of the absorption intensities of the difference band at 742/746 cm^{-1} shown in Fig. 6 in the range from 739 to 747 cm^{-1}. *x*-axis: intensity taken from the spectrum in Fig. 4 *a* (A_h-spectrum); *y*-axis: intensity taken from the spectrum in Fig. 4 *b* (A_v-spectrum). The slope defines a dichroic ratio of $R = 1.08$.

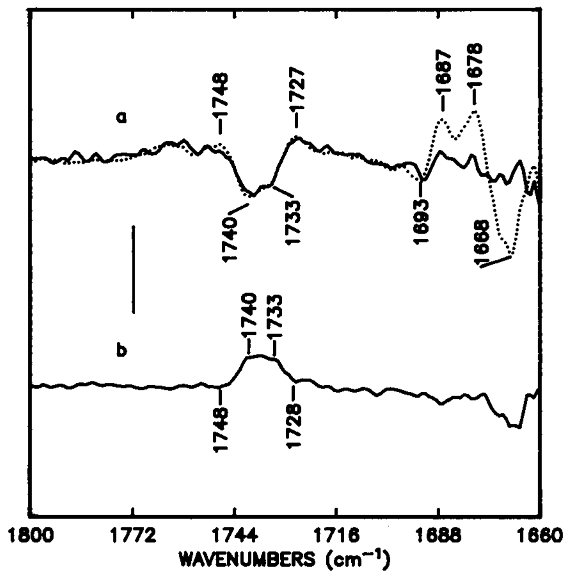

FIGURE 8 Polarized measurements of the BR-L transition induced by light with wavelengths above 610 nm at 170 K in H_2O. Spectral range of absorption of protonated carboxyl groups and high frequency amide I vibrations. The spectra shown in the upper traces were induced by unpolarized actinic light and recorded with the plane of the sample tilted by 44° with respect to the incident IR-beam. The lower trace represents a photoselection experiment. (*a*) Solid line: A_h-spectrum; dotted line: A_v-spectrum. (*b*) Dichroic difference spectrum. The bar indicates an absorption change of $3*10^{-3}$ and $3.3*10^{-4}$ absorbance units in *a* and *b*, respectively.

trum. Their bands overlap in BR_{568} around 1,740 cm^{-1} and become more separated in L (1,748 and 1,728 cm^{-1}). Fig. 8 shows that m_{ir} of both vibrations is similar with respect to Φ, which is ~70° as evidenced from the inversion of the bands at 1,740–1,733 cm^{-1} in the dichroic difference in Fig. 8 *b* (*lower trace*) as compared to the solid line of Fig. 8 *a* (*upper trace*), which coincides with an unpolarized measurement. In L, both vibrations exhibit $\Phi \sim 45°$, because the positive lobes at 1,748 and 1,728 cm^{-1} visible in Fig. 8 *a* have disappeared in the dichroic difference in Fig. 8 *b*. A somewhat smaller reorientation is observed with respect to θ: M_{ir} of the mode at 1,740 cm^{-1} exhibits a larger *z*-component ($\theta \sim 41°$) than that of 1,733 cm^{-1} ($\theta = 55°$). Both transition moments increase their *z*-components upon formation of L in which they are characterized by angles θ of 37° (1,748 cm^{-1}) and 44° (1,727 cm^{-1}). Beside these spectral changes, two highly dichroic bands of the L-intermediate are visible at 1,687 and 1,678 cm^{-1} in Fig. 8 *a* which are poorly resolved in the A_h spectrum (*solid line*) but become distinct in the A_v spectrum (*dotted line*). The dichroic ratio of both of them is > 3. Therefore, M_{ir} of these modes is completely oriented along the *z*-axis. For BR_{568}, only the absorption at lower frequency is well resolved (1,668 cm^{-1}). Again, it is polarized along the *z*-axis. The mode at higher frequency shows in BR_{568} a weak absorption around 1,690 cm^{-1} which (in contrast to the corresponding L-absorption) is equally visible in both A_h and A_v. Therefore, M_{ir} of this vibration reorients during the BR-L transition, thereby maximizing its *z*-component.

DISCUSSION

For an interpretation of the data presented in terms of molecular geometries, the studied vibrations have to be assigned to atomic groups on BR. FTIR-difference spectroscopy has the advantage of observing both chromophore and protein vibrations. On the other hand, the number of difference bands is large and a distinction between chromophore and protein absorption is difficult to achieve. This distinction can be facilitated by comparison with resonance Raman spectra of BR and its intermediates because only chromophore bands contribute to such spectra. In this study, we use the assignments of chromophore modes for light and dark-adapted BR derived by (20, 21). Their results are incorporated in Table I which summarizes the frequencies and polarizations of the studied modes in all-*trans* and 13-*cis*,15-syn BR and in the K- and L-intermediate. Due to different selection rules, Raman active modes cannot a priori be identified with IR-active modes based solely on identical frequencies. However, the resonance Raman assignments of the chromophore HOOPs marked in Table I could be confirmed in our earlier FTIR measurements by use of PM reconstituted with $^{12}C/^{13}C$ and $^1H/^2H$ substituted retinals (data not shown).

Localization of single bond torsions of the retinal chromophore in different BR states

Before discussing the orientation of chromophore HOOP modes in more detail, we want to point out the purpose and limits of a quantitative analysis. The measured Φ-values can be used to classify the corresponding HOOP vibrations into three classes. The first class consists of vibrations with $\Phi > 70°$, the second is characterized by $35° < \Phi < 55°$ and the third class is composed of HOOP modes with $\Phi < 20°$. The difference between these ranges are well outside the experimental error, including all polarization losses (see materials and methods). Although the accuracy of the measurements is good enough to obtain the more precise values of Table I, we restrict our structural interpretation to the rough classification of Φ values as defined. In view of our quantum chemical calculations, the three classes of HOOP modes correlate with planar or almost planar geometries (first class), moderately twisted C—C=C—C fragments (second class) and strongly distorted parts of the chromophore (third class). Our aim is to demonstrate the potential of polarized FTIR-spectroscopy to evidence the coexistence of planar and distorted regions within a given isomeric state of the retinal rather than to elucidate exact angles of torsions around C—C single bonds from the obtained Φ-values. However, we state that the relative degree of single bond torsions is indeed reflected by the classification of HOOP modes.

As explained in materials and methods, Φ is the angle between m_{ir} and m_{el}, i.e., between the projections of M_{ir} and M_{el} onto the plane of the sample. The question arises whether the real angle Φ' between M_{ir} and M_{el} differs from Φ to an amount that renders the classification of HOOP modes inapplicable. It is easy to prove that $\tan \Phi = \tan \Phi' \cos \delta_2/\cos \delta_1$ with δ_1 the tilt angle between M_{el} and the PM which is 19 ± 4° (31). δ_2 is the deviation of the average retinal plane in BR_{568} from the perpendicular orientation relative to the PM which is 0° ± 20° according to the presented data on the $C_7{=}C_8$ HOOP and our previous study (7). As $\Phi = \Phi'$ for 0° and 90° it is the second class of HOOP modes in which Φ differs maximally from Φ'. With the given values of δ_1 and δ_2 the maximal deviation between Φ and Φ' is only ±3°. The following structural interpretations of the data exclusively rely on the described classification of measured Φ-values and on the "rule of thumb" outlined in the introduction. We consider the thorough quantum-chemical studies (7, 8) to provide sufficient evidence for the validity of that rule.

According to such calculations for a planar protonated retinal Schiff base, M_{ir} of a HOOP mode (with the hydrogens trans of the C=C double bond) is expected to be directed along the normal of the molecular plane, whereas torsions around neighboring C—C single bonds increase the in-plane component (7). Therefore, an ideal HOOP vibration of the chromophore is characterized by $\Phi = 90°$ in contrast to $\Phi < 90°$ for HOOP modes in twisted regions of the retinal chromophore. The first information to be drawn from Table I is the occurrence of large deviations from the perpendicular orientation. They not only vary with respect to the position of the corresponding H-atom, but also depend on the intermediate in which the HOOP mode is observed. We find only the $C_7{=}C_8$ HOOP as an ideal HOOP vibration in all the BR-states investigated except K. From our previous study, we can conclude that local planarity is conserved around the $C_7{=}C_8$ double bond in light and dark-adapted BR as well as in L. Because of the ideal polarization of this HOOP mode, it is well suited to monitor the position of the local retinal plane with respect to the plane of the PM. The value of $\theta \sim 90°$ confirms our earlier results, in which we determined the average retinal plane of light-adapted BR to be approximately perpendicular to the PM (7). The results presented here demonstrate that the $C_6—C_7=C_8—C_9$ part of the chromophore, i.e., adjacent to the ionone ring, keeps this planar orientation irrespective of the isomeric state, i.e., all-*trans* in light-adapted BR, 13-*cis*,15-syn in the 13-*cis* component of dark-adapted BR or 13-*cis*,15-anti in L.

In the K-photoproduct, large single bond torsions must be inferred from our measurements because the chromophore HOOP modes are polarized nearly parallel to the retinal axis. The torsions include the $C_6—C_7=C_8—C_9$ part, which, after thermal relaxation to L, adopts again a planar configuration. However, the value of $\Phi = 45°$ for the $C_{11}=C_{12}$ HOOP evidences remaining torsions in the $C_{10}—C_{11}=C_{12}—C_{13}$ fragment of L. Therefore, the long-lived perturbations of the chromophore/protein interaction upon photoisomerization are localized in the terminal part of the chromophore environment rather than in the vicinity of the ionone ring, whereas the primary event evokes distortions of the entire chromophore. This corroborates conclusions drawn from BR-L measurements in ^2H_2O which indicate a significant torsion around the $C_{14}—C_{15}$ single bond in L (7).

Regarding the HOOP polarizations in light- and dark-adapted BR, the most striking result is the gain of planarity in the $C_{10}—C_{11}=C_{12}—C_{13}$ region of the chromophore upon dark-adaptation. This is monitored by the change in polarization of the $C_{11}=C_{12}$ HOOP from $\Phi = 45°$ in BR_{568} (959 cm^{-1}) to $\Phi > 70°$ in BR_{548} (956 cm^{-1}). It confirms our former conclusion that the all-*trans* chromophore of light-adapted BR is not completely planar. However, local torsions are also present in the 13-*cis*,15-syn chromophore of dark-adapted PM. The vibration at 800 cm^{-1} is assigned to the C_{14} HOOP (20) and is found to be polarized almost parallel to the retinal axis (Table I). This argues for a large twist around the $C_{14}—C_{15}$ single bond (comparable to those of the thermally not relaxed chromophore in K!) in this thermally relaxed chromophore state.

Our results on the chromophore geometry agree well with resonance Raman studies, in which high intensities of HOOP vibrations of K, BR_{548} ($C_{14}—C_{15}$ HOOP) and the early photoproduct of rhodopsin, i.e., bathorhodopsin were interpreted to be indicative of a distorted chromophore (19, 20, 22). A similar correlation between the intensity of a chromophore HOOP mode and molecular distortions seems to exist for the IR-active vibrations. M_{ir} of every intense HOOP vibration has a large component parallel to M_{el}, whereas all ideally polarized HOOPs possess low IR intensity. This is in accordance with quantum chemical calculations (7) which predict coupling of the HOOP vibrations to in-plane modes in twisted geometries. Due to the charge alternation along the polyene chain, this coupling increases the participation of charge movements in the normal mode, thereby increasing its IR activity. Correspondingly, the change from a pure or only slightly distorted HOOP mode to a considerably distorted HOOP in an FTIR difference spectrum would be visualized as the depletion of a weak absorption band and the rise of an intense one. As a result, only a positive absorption, instead of a more or less symmetrical difference band, should show up. This is exactly the case for the BR-K spectrum (Fig. 1) and holds for the band at 800 cm^{-1} in the light–dark-adaptation spectrum (Fig. 3), too.

Orientation of amino acid side chains and comparison with the three-dimensional structure of BR

The difference band at 742/746 cm^{-1}, present in all difference spectra, has been assigned to a HOOP vibration of Trp 86 which undergoes a frequency shift, possibly by altered H-bonding to the indolyl nitrogen (23, 24). In a first approximation, M_{ir} should be perpendicular to the plane of the Trp residue. Our results of polarized light–dark-adaptation measurements indicate nearly orthogonality between the normal of the Trp 86 plane and m_{el} of the chromophore in light-adapted BR. However, the plane of Trp 86 cannot be parallel to the plane of the all-*trans* retinal Schiff base. This can be concluded from the large z-component of the 742/746 cm^{-1} mode as evidenced by the dichroic ratio taken from Fig. 7. With the average plane of the all-*trans* retinal chromophore being perpendicular to that of PM, the data predict an angle of 54° between the plane of the chromophore and that of Trp 86. According to our results, the orientation of Trp 86 in light-adapted BR then essentially persists in K, L and dark-adapted BR and differs from that suggested by (23). However, with respect to the BR_{568} state at different temperatures, the data for the Trp 86 vibration are less consistent and one might suspect an influence of temperature on the orientation of M_{ir} of this mode. θ is determined to 33° at 80 K, to a value greater than 80° at 170 K and to 46° at 280 K. However, the small value of 0.6 of the dichroic ratio obtained at 170 K is inconsistent with a refractive index of 1.7, which limits R to values greater than 0.8. Therefore, a refractive index of 1.2 had to be assumed, which would contradict published values. In addition the evaluation of the other modes is consistent with $n = 1.7$. Thus the low value of the dichroic ratio must be explained in a different way. An overlap of the band at 742 cm^{-1} with an unknown absorption of the L-intermediate, causing a positive band near 742 cm^{-1} can be the reason for the unusual low value of the apparent dichroic ratio. The superimposed band must be supposed to be caused by a transition moment with a large z-component. In this case, the negative band at 742 cm^{-1}

is compensated to a larger extent in A_v than in A_h, thereby diminishing the dichroic ratio of the absorption of Trp 86 in BR_{568}. In photoselection measurements, the sample is not tilted and, consequently, absorption due to M_{ir} with a large z-component is very weak. For this reason, the influence of the overlapping band of the photoproduct on the evaluation of the Trp 86 vibration in BR_{568} at 742 cm^{-1} should be less in the photoselection experiments. Therefore, the conclusion that a temperature dependence of the orientation of M_{ir} of Trp 86 in BR_{568} is well reflected by the alteration of Φ from 62° at 280 K to $\sim 45°$ at low temperatures (80 K and 170 K corresponding to K and L measurements) is still correct. However, the true value of θ of this mode at low temperature can only be extracted from the BR-K difference spectrum, which, in contrast to the BR-L difference spectrum, allows the undisturbed observation of the Trp 86 vibration and predicts $\theta = 33°$. Here, θ is decreased by 13° upon cooling the sample. One should bear in mind that, due to the large z-component of the HOOP-vibration of Trp 86, only small rearrangements of this residue can cause considerable alterations in Φ.

The difference band at 757/751 cm^{-1} in BR-L spectra is caused by another Trp residue (23) which, however, could not be assigned to a specific Trp of the sequence. Our data show that in this case the normal of the molecular plane of Trp is tilted by 45° from the retinal axis but exhibits the same tilt angle with respect to the z-axis as Trp 86. Almost no alteration of this arrangement is found in L. From the fact, that the 757/751 cm^{-1} difference band is only seen in L and M (data not shown) one could conclude that the corresponding Trp is not directly influenced by the isomeric state of the chromophore in contrast to Trp 86 which gives rise to a difference band whenever an all-*trans* to 13-*cis* isomerization occurs.

The band at 833 cm^{-1} has been assigned to Tyr 185 (25). Based on a comparison with resonance Raman studies on Tyr residues and related molecules in model compounds, it was assigned to a fermi resonance between the ring-breathing vibration and an overtone of an out-of-plane-bending (HOOP) vibration (26, 27). However, for the IR-active modes of p-cresol a strong mode at 817 cm^{-1} was assigned to a pure HOOP vibration (28, 29). We carried out FTIR studies on p-cresol and found the frequency of this vibration to be sensitive to solvent. In carbon tetrachloride, we observed the absorption at 817 cm^{-1}, whereas in DMSO it is shifted to 830 cm^{-1} due to hydrogen bonding of the OH group to the solvent (data not shown). Therefore, we attribute the absorption of light-adapted BR at 833 cm^{-1} to a HOOP mode of Tyr 185 in a hydrogen bonded state. Taking the planarity of the Tyr residue into account, the polarization of this HOOP vibration is expected to be perpendicular to the molecular plane. The polarized FTIR data show that Tyr 185 is oriented in a way in which its molecular plane is parallel to that of all-*trans*-retinal in light-adapted BR. It remains in this orientation in K, because the polarization of the HOOP, which is now seen at 829 cm^{-1} is still perpendicular to m_{el} and lies in the plane of the PM. In L, the perturbation of this residue is small. Only weak difference bands are observed. Similarly, in dark-adapted BR it is not clear where to localize the HOOP mode. Therefore, no detailed description of the orientation of Tyr 185 can be given for the two last-mentioned BR states. However, the small absorbance changes exclude significant alterations in the environment of this residue which renders any considerable reorientations unlikely. The assignment of the 833 cm^{-1} band to a HOOP vibration is supported by the orientation of M_{ir} of a mode at 1,277 cm^{-1}. The latter has been assigned to a mode of Tyr 185 which contains C—O stretching character (25, 30) and which can be assumed to be oriented in the plane of the ring. From our K-measurements, we find $\Phi = < 10°$ (data not shown). Therefore, M_{ir} of the stretch and HOOP vibration of Tyr 185 are perpendicular to each other as expected.

The recent publication of the three dimensional structure of BR derived from electron cyro-microscopy (31) enables us to compare our results with the orientations of molecular planes and directions of chemical bonds suggested by the electron density map. The molecular environment of the chromophore according to the three dimensional model is shown in Fig. 9 viewed from the cytoplasmic side of the PM. With respect to the orientation of the average retinal plane, the three-dimensional model had to rely on results which had been obtained by other methods. It has been shown by polarized FTIR spectroscopy on native BR_{568} that the average plane of the chromophore is nearly perpendicular to the PM (7). This is supported by the presented data on the $C_7{=}C_8$ HOOP in BR_{568}. M_{el} is tilted by 19° out of the plane of the PM (32). The direction of this tilt leads to an orientation of the C=C double bonds essentially in the plane of the PM (7) (i.e., the vector connecting the Schiff base and the ionone ring points towards the same membrane surface as the N→H bond in agreement with conclusions from neutron diffraction [33]). Both conclusions from the polarized FTIR-data are corroborated by the comparison of the linear dichroism of native BR_{568} with that of light-adapted BR regenerated with 3,4 dehydroretinal (34). In addition, the ionone ring points toward the extracellular side of the PM (35). These results are of special interest, because they determine the intramolecular direction of

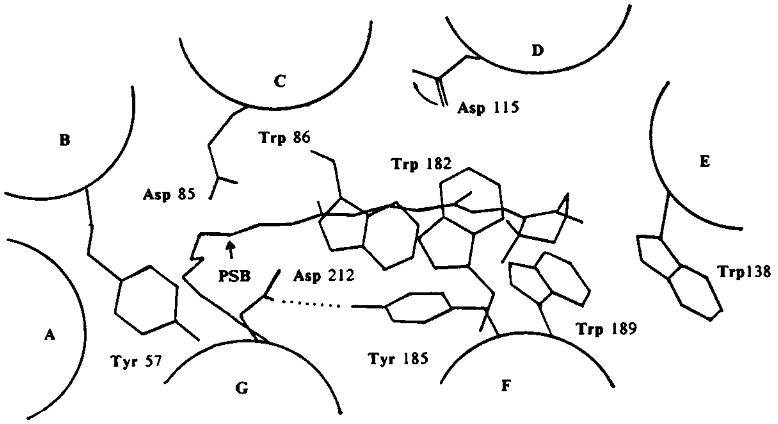

FIGURE 9 Molecular environment of the retinal chromophore of BR$_{568}$ based on electron density evaluation. View onto the cytoplasmic surface of the PM. The region below and above the chromophore comprises a slice of 7 A thickness. Trp 182 is above, Trp 86 below the chromophore (figure taken from 31 and simplified). Additional features, which correspond to the results of the FTIR-measurements, are the hydrogen bond between Tyr 185 and Asp 212 and the identification of the C=O bond of protonated Asp 115. The latter reorients upon formation of the L-intermediate as is indicated by the arrow. A similar reorientation can be concluded for the protonated Asp 96, which is located above the protonated Schiff base, but is not part of the molecular slice depicted. PSB: protonated Schiff base; A–G: designation of the transmembrane helices.

the translocation of the Schiff Base upon photoisomerization, i.e., towards Asp 85 and Asp 212 according to the three-dimensional model.

The fit of the primary amino acid sequence into the electron density map has allowed an accurate determination of the position of aromatic side chains within the membrane profile but the orientation of the corresponding groups has remained uncertain in many cases. On the other hand, polarized FTIR difference spectroscopy cannot evaluate atomic distances but has proven to be well suited to determine the orientation of molecular planes and chemical bonds (7, 10–12, 17). Therefore, the IR-data represent supplementary information with respect to the protein structure. In the case of Tyr 185, the molecular shape restricts the orientation of the side chain to a parallel arrangement of the ring and the polyene plane of the retinal to fit into the electron density. Our results reproduce the same orientation for this well determined side chain. Furthermore, we can confirm the suggested orientation of Trp 86 which deviates considerably from the parallel arrangement found for Tyr 185. Also, the structural flexibility of parts of the protein can be estimated by polarized FTIR-difference spectroscopy. Apart from the effect of temperature on the Trp 86 HOOP mode in BR$_{568}$, the lack of distinct reorientations of M_{ir} upon photoisomerization demonstrates that Tyr 185, Trp 86 and the second Trp perturbed in L (and M) reflect a rigid retinal binding pocket rather than highly mobile parts of the protein. Because the high frequency of the Tyr 185 HOOP mode indicates strong hydrogen bonding of this residue, it is likely that this hydrogen bond contributes to the rigidity. The three dimensional model argues for hydrogen bonding of Tyr 185 to Asp 212 as indicated in Fig. 9.

In contrast to the discussed protein modes, M_{ir} of Asp 96 and Asp 115 exhibit distinct reorientation upon formation of L-intermediate. For both transition moments, Φ decreases by 20°–30° and the z-components are slightly enlarged. The same values for θ and Φ are observed when measured in ^2H_2O (7). This indicates minor coupling effects of the O—H bending vibration to the C=O stretch with respect to the orientation of M_{ir} of the latter. MNDO calculations for model compounds carried out according to the procedures described in (7) reproduce this observation. They predict a reorientation of M_{ir} for the C=O stretch by $< 1°$ upon deuteration. Therefore, the alteration in Φ of the carboxyl groups during the BR-L transition reflects a molecular rearrangement rather than alterations in coupling caused by environmental changes. This rearrangement could be a rotation around the 3C—4C single bond or a proton exchange between the two oxygens of the carboxyl group. The quantum chemical calculations on protonated acetic acid predict M_{ir} of the C=O stretching vibration to deviate by 15° (in the plane of the carboxyl group but outside of the O,C,O angle) from the direction of the C=O bond. Our polarized FTIR-data argue that in the three dimensional model the C=O bonds of Asp 96 and 115 in BR$_{568}$ are represented by those branches that point towards the retinal. Only Asp 115 is part of the molecular "slice" depicted in Fig. 9 and its C=O bond is indicated according to the results. The ease by which the FTIR-data on Asp 115 can be incorporated into the three dimensional model supports the proposed arrangement of helix D which is the least certain part of the model. A similar orientation of Asp 96 (on helix C) can be inferred from the polarization measurement and is, indeed, in agreement with the three-dimensional model. Formation of L causes the molecular reorientations of both carboxyl groups which might participate in the formation of a proton channel through the protein.

Taking the data of the polarization of chromophore and protein bands together, we conclude that dynamics of the chromophore geometry within a rather rigid binding site play an important role up to the formation of L intermediate. The functional relevance of the protein structure can be viewed as imposing sterical constraints on the photoisomerized retinal chromophore, thereby directing thermal relaxation of a highly distorted 13-*cis* isomer towards a 13-*cis* isomer with single bond torsions localized in the Schiff base region. These structural details of the retinal geometry in L may be a prerequisite for the deprotonation of the Schiff base in the following M intermediate (9).

Stimulating discussions with H. C. Spatz and W. Kreutz are gratefully acknowledged.

This work has been supported by the Deutsche Forschungsgemeinschaft grant SFB 60 G9.

Received for publication 30 January 1991 and in final form 19 June 1991.

REFERENCES

1. Stoeckenius, W., R. H. Lozier, and R. A. Bogomolni. 1979. Bacteriorhodopsin and the purple membrane of halobacteria. *Biochim. Biophys. Acta.* 505:215–278.
2. Stoeckeinius, W., and R. A. Bogomolni. 1982. Bacteriorhodopsin and related pigments of halobacteria. *Annu. Rev. Biochem.* 51:587–616.
3. Lozier, R. H., R. A. Bogomolni, and W. Stoeckenius. 1975. Bacteriorhodopsin: a light-driven proton pump in halobacterium halobium. *Biophys. J.* 15:955–962.
4. Curry, B., A. Broek, J. Lugtenburg, and R. A. Mathies. 1982. Vibrational analysis of all-*trans*-retinal. *J. Am. Chem. Soc.* 104:5274–5286.
5. Curry, B., I. Palings, A. Broek, J. A. Pardoen, P. P. J. Mulder, J. Lugtenburg, and R. A. Mathies. 1984. Vibrational analysis of 13-*cis*-retinal. *J. Phys. Chem.* 88:688–702.
6. Curry, B., I. Palings, J. A. Pardoen, J. Lugtenburg, and R. A. Mathies. 1985. Vibrational analysis of retinal isomers. *Adv. Infrared Raman Spectrosc.* 12:115–124.
7. Fahmy, K., M. F. Großjean, F. Siebert, and P. Tavan. 1989. The photoisomerization in bacteriorhodopsin studied by FTIR linear dichorism and photoselection experiments combined with quantumchemical theoretical analysis. *J. Mol. Struct.* 214:257–288.
8. Großjean, M. F., P. Tavan, and K. Schulten. 1990. Quantumchemical vibrational analysis of the retinal chromophore of bacteriorhodopsin. *J. Phys. Chem.* 94:8095–8069.
9. Schulten, K., and P. Tavan. 1978. A mechanism for the light driven proton pump of Halobacterium halobium. *Nature (Lond.).* 272:85–86.
10. Breton, J., and E. Nabedryk. 1989. Light-induced polarized Fourier transform infrared spectroscopy of bacteriorhodopsin: a study of the M_{412} intermediate by photoselection: *Biochim. Biophys. Acta.* 973:13–18.
11. Earnest, T. N., P. Roepe, M. S. Braiman, J. Gillespie, and K. J. Rothschild. 1986. Orientation of the bacteriorhodopsin chromophore probed by polarized Fourier transform infrared difference spectroscopy. *Biochemistry.* 25:7793–7798.
12. Nabedryk, E., and J. Breton. 1986. Polarized Fourier transform infrared (FTIR) difference spectroscopy of the M_{412} intermediate in the bacteriorhodopsin photocycle. (*FEBS Fed. Eur. Biochem. Soc. Lett.*) 202:356–360.
13. Oesterhelt, D., and W. Stoeckenius. 1974. Isolation of the cell membrane of halobacterium halobium and its fractionation into red and purple membrane. *Methods Enzymol.* 31:667–678.
14. Tokunaga, F., and T. G. Ebrey. 1978. The blue membrane: the 3-dehydroretinal-based artificial pigment of the purple membrane. *Biochemistry.* 17:1915–1922.
15. Lugtenburg, J. 1985. Synthesis of ^{13}C-labelled retinals. *Pure Appl. Chem.* 57:753–762.
16. Pardoen, J., C. Winkel, P. Mulder, and J. Lugtenburg. 1984. Synthesis of retinals labelled at positions 14 and 15 (with ^{13}C and/or ^{2}H). *Recl. Trav. Chim. Pays-Bas.* 103:135–141.
17. Rothschild, K. J., and N. A. Clark. 1979. Polarized infrared spectroscopy of oriented purple membrane. *Biophys. J.* 25:473–488.
18. Henniker, C. J. 1973. Infrared refractive indices of some oriented polymers. *Macromol.* 6:514–514.
19. Braiman, M., and R. A. Mathies. 1982. Resonance Raman spectra of bacteriorhodopsin's primary photoproduct: evidence for a distorted 13-*cis* retinal chromophore. *Proc. Natl. Acad. Sci. USA.* 79:403–407.
20. Smith, S. O., J. A. Pardoen, J. Lugtenburg, and R. A. Mathies. 1987. Vibrational analysis of the 13-*cis*-retinal chromophore in dark-adapted bacteriorhodopsin. *J. Phys. Chem.* 91:804–819.
21. Smith, S. O., M. S. Braiman, A. B. Myers, J. A. Pardoen, J. M. L. Courtin, C. Winkel, J. Lugtenburg, and R. A. Mathies. 1987. Vibrational analysis of all-*trans*-retinal chromophore in light-adapted bacteriorhodopsin. *J. Am. Chem. Soc.* 109:3108–3125.
22. Eyring, G., B. Curry, A. Broek, J. Lugtenburg, and R. Mathies. 1982. Assignment and interpretation of hydrogen out-of-plane vibrations in the resonance Raman spectra of rhodopsin and bathorhodopsin. *Biochemistry.* 21:384–393.
23. Rothschild, K. J., D. Gray, T. Mogi, T. Marti, M. S. Braiman, L. J. Stern, and H. G. Khorana. 1989. Vibrational spectroscopy of bacteriorhodopsin mutants: chromophore isomerization perturbs tryptophan-86. *Biochemistry.* 28:7052–7059.
24. Roepe, P., D. Gray, J. Lugtenburg, E. M. M. Van den Berg, J. Herzfeld, and K. J. Rothschild. 1988. FTIR evidence for tryptophan perturbations during the bacteriorhodopsin photocycle. *J. Am. Chem. Soc.* 110:7223–7224.
25. Braiman, M. S., T. Mogi, L. J. Stern, N. R. Hackett, B. H. Chao,

H. G. Khorana, and K. J. Rothschild. 1988. Vibrational spectroscopy of bacteriorhodopsin mutants. I. tyrosine-185 protonates and deprotonates during the photocycle. *Proteins.* 3:219–229.

26. Rothschild, K. J., P. Roepe, P. L. Ahl, T. N. Earnest, R. A. Bogomolni, S. K. Das Gupta, C. M. Mulliken, and J. Herzfeld. 1986. Evidence for a tyrosine protonation change during the primary phototransition of bacteriorhodopsin at low temperature. *Proc. Natl. Acad. Sci. USA.* 83:347–351.

27. Siamwiza, M. N., R. C. Lord, M. C. Chen, T. Takamatsu, I. Hrada, H. Matsuura, and T. Shimanouchi. 1975. Interpretation of the doublet at 850 cm^{-1} and 830 cm^{-1} in the resonance Raman spectra of tyrosyl residues in proteins and certain model compounds. *Biochemistry.* 14:4870–4876.

28. Jakobson, R. J. 1965. The vibrational spectra of p-cresole. *Spectrochim. Acta.* 21:433–442.

29. Green, J. H., D. J. Harrison, and W. Kynaston. 1971. Vibrational spectra of benzene derivatives-XIV Mono substituted phenols. *Spectrochim. Acta.* 27A:2199–2217.

30. Dollinger, G., L. Eisenstein, Sh.-L. Lin, K. Nakanishi, and J. Termini. 1986. Fourier transform infrared difference spectroscopy of bacteriorhodopsin and its photoproducts regenerated with deuterated tyrosine. *Biochemistry.* 25:6524–6533.

31. Henderson, R., J. M. Baldwin, T. A. Ceska, F. Zemlin, E. Beckmann, and K. H. Downing. 1990. Model for the structure of bacteriorhodopsin based on high-resolution electron cryomicroscopy. *J. Mol. Biol.* 213:899–929.

32. Heyn. M. P., R. J. Cherry, and U. Müller. 1977. Transient and linear dichroism studies on bacteriorhodopsin: determination of the orientation of the 568-nm all-*trans* chromophore. *J. Mol. Biol.* 117:607–620.

33. Hauss, T., S. Grzesiek, H. Otto, J. Westerhausen, and M. P. Heyn. 1990. Transmembrane location of retinal in bacteriorhodopsin by neutron diffraction. *Biochemistry.* 29:4904–4913.

34. Lin, S. W., and R. A. Mathies. 1989. Orientation of the protonated retinal Schiff base group in bacteriorhodopsin from absorption linear dichroism. *Biophys J.* 56:653–660.

35. Huang, J. Y., and A. Lewis. 1989. Determination of the absolute orientation of the retinylidene chromophore in purple membrane by a second-harmonic interference technique. *Biophys. J.* 55:835–842.

36. Braiman, M. S., T. Mogi, T. Marti, L. J. Stern, H. G. Khorana, and K. J. Rothschild. 1988. Vibrational spectroscopy of bacteriorhodopsin mutants: light-driven proton transport involves protonation changes of asprartic acid residues 85,96 and 212. *Biochemistry.* 27:8516–8520.

37. Gerwert, K. 1986. Transduktion der Lichtenergie in Protonen-Transfer-Reaktionen beim Bacteriorhodopsin. Ph.D. thesis. Universität Freiburg, Germany.